J. Am. Chem. Soc. 1984, 106, 6254-6262

Vibrational Circular Dichroism of *trans*-1,2-Dideuteriocyclobutane. A Comparison of Fixed Partial Charge and Localized Molecular Orbital Theories with Different Force Fields

A. Annamalai,[†] T. A. Keiderling,*[†] and J. S. Chickos[‡]

Contribution from the Department of Chemistry, University of Illinois at Chicago, Chicago, Illinois 60680, and the Department of Chemistry, University of Missouri—St. Louis, St. Louis, Missouri 63121. *Received December 12, 1983*

Abstract: Vibrational circular dichroism and absorption spectra for *trans*-1,2-dideuteriocyclobutane in both gas phase and solution are presented and analyzed by using the effective charge and localized molecular orbital theories. In the C–H and C–D stretching regions both theories give similar VCD line shapes, but these, in turn, depend on the force field used. Calculations using the early force field by Lord and Nakagawa satisfactorily fit the C–H region but not the C–D region of the VCD spectrum. However, the ab initio force field of Banhegyi, Fogarasi, and Pulay gives results that fit the VCD of both regions better. The actual magnitudes obtained with the LMO model are high for both ϵ and $\Delta\epsilon$, but the $\Delta\epsilon/\epsilon$ values still approximate those found experimentally. The FPC model gives an adequate fit to both ϵ and $\Delta\epsilon$ with effective charges scaled to fit the absorption. Equal charges on all the hydrogens give the best absorption line shape, but the VCD line shape seems relatively insensitive to charge distribution. Other variations of the calculations are also discussed.

In recent years, we and other groups have demonstrated the experimental feasibility of measuring vibrational circular dichroism (VCD) over much of the infrared region.[1-5] Data obtained on a variety of molecules have demonstrated that VCD is very sensitive to details of molecular geometry. To make this structural sensitivity useful to chemists, a relationship between structure and spectra must be developed. While this might be accomplished by empirical comparison of VCD for a number of structurally similar compounds, as was done originally for electronic CD, a reliable theoretical model would have more generality. Several such theories have been proposed. This paper will address two of them, a simple effective or fixed partial charge (FPC) model as formulated by Schellman[6-8] and the more complex localized molecular orbital (LMO) model put forth by Nafie and coworkers.[9-11]

We and others have previously applied the FPC model to the study of C–H stretching motions of five- and six-member hydrocarbon rings with some success.[12-15] In these cases, it was possible to reproduce approximately the experimentally found VCD line shape by overlap of contributions from the CH$_2$ stretching modes. This agreement of model calculation with experiment was later attributed to a dipolar coupling of the asymmetric stretches of skewed, vicinal CH$_2$ groups which thus form an "inherently dissymmetric chromophore".[16] Such coupled-oscillator[17] effects have been shown to give rise to large VCD signals for modes such as carbonyl stretches which are characterized by high local symmetry and large transition dipoles.[18-21]

Application of the FPC model to other systems has been less successful. Vibrational modes involving heteroatoms (particularly those with lone pairs)[19,22-28] and π systems[12,19,26,27] often yield FPC calculated VCD that is much smaller than found experimentally. This is especially true of spectroscopically isolated modes in such systems, for example, as the C*–H modes of 2,2,2-trifluoro-1-phenylethanol[22] and alanine-*C*-d_3-*N*-d_2[25] and the O–H mode of 1-(dimethylamino)-2-propanol.[23] On the other hand, this array of calculations clearly points out which molecules should be appropriate for FPC-VCD study. The most obvious experimental choices are the saturated hydrocarbons—a prediction which is consistent with those cases above for which success of the FPC model has already been shown at some level.[12-15]

Nafie and co-workers have subsequently shown that, in the C–H stretching region, the LMO model gives calculated VCD which is qualitatively similar to that of the FPC model for 3-methylcyclohexanone.[11] The FPC results, in turn, agree with experiment.[14] But, more importantly, the LMO model gives a reasonable fit to experimental VCD for other molecules where the FPC model fails.[10,29] It has been further noted that the LMO model avoids

---

[†] University of Illinois at Chicago.

[‡] University of Missouri—St. Louis.

(1) Keiderling, T. A. *Appl. Spectrosc. Rev.* **1981**, *17*, 189.

(2) Nafie, L. A. *Adv. Infrared Raman Spectrosc.* **1984**, *11*, 49. Nafie, L. A. *Vib. Spectra Struct.*, *10*, **1981**, 153. Nafie, L. A.; Diem, M. *Acc. Chem. Res.* **1979**, *12*, 296.

(3) Stephens, P. J.; Clark, R. In "Optical Activity and Chiral Discrimination"; Mason, S. F.; Ed.; Reidel: Dortrecht, 1979.

(4) Mason, S. F. *Adv. Infrared Raman Spectrosc.*; *8*, **1980**, 283.

(5) Polavarapu, P. L. *Vib. Spectra Struct.*, in press.

(6) Schellman, J. A. *J. Chem. Phys.* **1973**, *58*, 2882; **1974**, *60*, 343.

(7) Deutsche, C. W.; Moscowitz, A. *J. Chem. Phys.* **1968**, *49*, 3257; **1970**, *53*, 2630.

(8) Cohan, N. V.; Hameka, H. F. *J. Am. Chem. Soc.* **1966**, *88*, 2136.

(9) Nafie, L. A.; Walnut, T. H. *Chem. Phys. Lett.* **1977**, *49*, 441. Walnut, T. H.; Nafie, L. A. *J. Chem. Phys.* **1977**, *67*, 1501.

(10) Nafie, L. A.; Polavarapu, P. L. *J. Chem. Phys.* **1981**, *75*, 2935.

(11) Polavarapu, P. L.; Nafie, L. A. *J. Chem. Phys.* **1981**, *75*, 2945.

(12) Keiderling, T. A.; Stephens, P. J. *J. Am. Chem. Soc.* **1979**, *101*, 1396.

(13) Singh, R. D.; Keiderling, T. A. *J. Chem. Phys.* **1981**, *74*, 5347. *J. Am. Chem. Soc.* **1981**, *103*, 2387.

(14) Polavarapu, P. L.; Nafie, L. A. *J. Chem. Phys.* **1980**, *73*, 1567.

(15) Marcott, C.; Scanlon, K.; Overand, J.; Moscowitz, A. *J. Am. Chem. Soc.* **1981**, *103*, 483.

(16) Laux, L.; Pultz, V.; Abbate, S.; Havel, H. A.; Overend, J. A.; Moscowitz, A.; Lightner, D. A. *J. Am. Chem. Soc.* **1982**, *104*, 4276.

(17) Holzwarth, G.; Chabay, I. *J. Chem. Phys.* **1972**, *57*, 1632.

(18) Narayanan, U.; Keiderling, T. A. *J. Am. Chem. Soc.* **1983**, *105*, 6406. Su, C. N.; Keiderling, T. A. *Ibid.* **1980**, *102*, 511.

(19) Su, C. N. Ph.D. Thesis, University of Illinois at Chicago, 1982.

(20) Heintz, V. J.; Keiderling, T. A. *J. Am. Chem. Soc.* **1981**, *103*, 2395.

(21) Singh, R. D.; Keiderling, T. A. *Biopolymers* **1981**, *20*, 237. Lal, B. B.; Nafie, L. A. *Ibid.* **1981**, *21*, 2161. Sen, A. C.; Keiderling, T. A. *Ibid.* **1984**, *23*, 1519, 1545.

(22) Faulkner, T. R.; Moscowitz, A.; Holzwarth, G.; Hsu, E. C.; Mosher, H. S. *J. Am. Chem. Soc.* **1974**, *96*, 252. Faulkner, T. R. Ph.D. Thesis, University of Minnesota, Minneapolis, 1976. Faulkner, T. R.; Marcott, C.; Moscowitz, A.; Overend, J. *J. Am. Chem. Soc.* **1977**, *99*, 8160.

(23) Marcott, C. Ph.D. Thesis, University of Minnesota, Minneapolis, 1979.

(24) Laux, L. J.; Abbate, S.; Pultz, V. M.; Ferber, S. D.; Overend, J.; Moscowitz, A. 35th Symposium on Molecular Spectroscopy, Columbus, OH, 1980; paper RG4.

(25) Lal, B. B.; Diem, M.; Polavarapu, P. L.; Oboodi, M.; Freedman, T. B.; Nafie, L. A. *J. Am. Chem. Soc.* **1982**, *104*, 3336.

(26) Su, C. N.; Keiderling, T. A. *Chem. Phys. Lett.* **1981**, *77*, 494.

(27) Heintz, V. J.; Annamalai, A.; Keiderling, T. A., unpublished results.

(28) Havel, H. A. Ph.D. Thesis, University of Minnesota, Minneapolis, 1981.

0002-7863/84/1506-6254$01.50/0

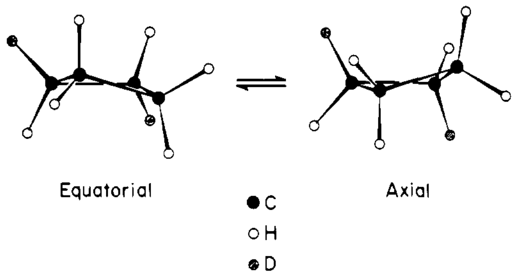

Figure 1. Two conformers of *trans*-1(*R*),2(*R*)-dideuteriocyclobutane used in VCD calculations. Note the opposite chirality of the CH_2CH_2 groups in the two conformers.

the need for the parameterization, i.e., the effective charges, required in the FPC model.[10] Such an improvement comes at considerable cost since the LMO calculations require two MO and orbital localization calculations for distorted geometries corresponding to each normal mode of interest (vide infra). With large molecules, this procedure could become prohibitively expensive. For this reason, to date, all LMO calculations have been done at the level of the CNDO approximation.

An alternative method of calculating the LMO-VCD based on the electric field gradient methods of Kormonicki[30] has been proposed,[31] but this alternative results in unreliable VCD with the approximate wave functions we use.[32] It should be noted that other calculational schemes have also been developed to account for the electronic contribution to VCD. These include models which correct for charge-flow contributions[33] and lone-pair effects,[23] as well as those that use atomic polar tensor methods[34] and nonlocalized MO techniques.[32] Nafie and Freedman[32] have recently compared the strengths and weaknesses of these models and have shown each to be, at some level, encompassed by the LMO model. Hence, in this paper, we will restrict ourselves to just the FPC and LMO approaches to VCD which then allows comparison of the most simple and most complex ground-state models currently available in computational form. Clearly, it would be advantageous to define situations in which the simple, inexpensive FPC model can be reliably used. This paper is one of a series aimed at developing such insight into the strengths and weaknesses of the FPC-VCD model.[12,13]

In general, previous attempts to compare VCD theory and experiment have involved the study of relatively complicated molecules. The experimental necessity that these molecules be both chiral and readily resolvable into optical isomers has, in general, prevented study of many simple molecules. Unfortunately, most of the molecules chosen previously have a variety of possible conformations which must be properly taken into account. Operationally, this involves the performance of several calculations and the combination of the results after weighting by the relative conformer populations. In addition, these low-symmetry molecules must be studied with, at best, an approximate force field transferred from studies of other systems. Extensively developed force fields are generally available only for simple, relatively high-symmetry molecules for which various isotopic species can be obtained.

In this paper, we have overcome some of the above-mentioned problems by obtaining and studying the VCD of *trans*-1(*R*),2(*R*)-dideuteriocyclobutane. The primary advantage of this molecule is that it is a small, saturated hydrocarbon without heteroatoms. This molecular simplicity facilitates extensive theoretical analyses and comparison of different models. The data presented here may, in fact, prove to be the hydrocarbon bench mark against which future theories can be tested. While cyclobutane does have conformational flexibility, the *trans*-dideuterio isomer is limited to two puckered conformations, presumably of equal energy, which have a single geometry now established by both experiment and theory.[35–38] Hence, it is clear what molecular structure to choose in order to proceed with the various calculations. The fact that two conformers exist even poses an additional advantage. The two CH_2 groups (Figure 1) in the trans isomer form a chiral group[16] which has the opposite sense in the two conformers. Contributions to the VCD from the dipolar coupling of these CH_2 groups in one conformer should then be canceled by those in the other conformer. Thus, the equal admixture of the two conformations expected to be present at room temperature gives a more severe test of the theories than was previously obtained with single-conformation, six-member ring hydrocarbons.

Perhaps the most important advantage of studying the VCD of cyclobutane is that extensive studies of its infrared and Raman spectra[39–43] have resulted in the development of force fields[44–46] which we can directly couple without modification to FPC and LMO VCD calculations. Availability of vibrational data for several isotopic species allows development of a force field which can be conventionally held to be reliable. Previously published vibrational data for C_4H_8 and C_4D_8[39,42] combined with the data for both *cis*- and *trans*-1,2-$C_4H_6D_2$, obtained in our laboratories, have been used to optimize both the original Lord and Nakagawa (L&N)[44] force field and the Banhegyi, Fogarasi, and Pulay (BFP)[45] ab initio force field. Optimization of the force fields has involved an improved fit of the original and subsequently assigned fundamental frequencies as proposed by BFP[45] and Aleksanyan and Antipov.[41] Details of our assignments for the *cis*- and *trans*-1,2-$C_4H_6D_2$ and optimization of the force field will be published separately.[47]

It should be explicitly noted that this study of cyclobutane VCD is possible due to the fact that its optical activity results solely from isotopic substitution. Such isotopic VCD has previously been reported for α-deuterated cyclohexanones,[48] phenylethanes,[28] and neopentyl-*1-d* chloride.[24,49] In all cases, including the present one, VCD signals are easily measurable while, typically, the electronic CD and ORD spectra are somewhat difficult to measure. Due to this reversal from the usual relative sensitivities, VCD can be a very useful monitor of isomeric purity for mechanistic studies. We will separately report on such an application of VCD. Finally, it can be noted that this is one of the first reports of gas-phase VCD.[50]

---

(29) Freedman, T. B.; Diem, M.; Polavarapu, P. L.; Nafie, L. A. *J. Am. Chem. Soc.* **1982**, *104*, 3343.

(30) Kormonicki, A.; McIver, J. W. *J. Chem. Phys.* **1979**, *70*, 2014.

(31) Polavarapu, P. L. *J. Chem. Phys.* **1982**, *72*, 2273. Polavarapu, P. L.; Chandrasekhar, J. *Chem. Phys. Lett.* **1981**, *84*, 587. Nafie, L. A.; Freedman, J. B. *J. Chem. Phys.* **1981**, *75*, 4847.

(32) Freedman, T. B.; Nafie, L. A. *J. Phys. Chem.* **1984**, *88*, 496.

(33) Abbate, S.; Laux, L.; Overend, J.; Moscowitz, A. *J. Chem. Phys.* **1981**, *75*, 3161. Moskovits, M.; Gohin, A. *J. Phys. Chem.* **1982**, *86*, 3947.

(34) Freedman, T. B.; Nafie, L. A. *J. Chem. Phys.* **1983**, *78*, 27.

(35) Skancke, P. N.; Forgarasi, G.; Boggs, J. E. *J. Mol. Struct.* **1980**, *62*, 259.

(36) Cremer, D. *J. Am. Chem. Soc.* **1977**, *99*, 1307.

(37) Meiboom, S.; Snyder, L. C. *J. Am. Chem. Soc.* **1967**, *89*, 1038; *J. Chem. Phys.* **1970**, *52*, 3857.

(38) Takabayoshi, F.; Kambara, H.; Kuchitsu, K. 7th Austin Symposium on Gas Phase Molecular Structure, Austin, TX, March 1978. Almennigen, A.; Bastiansen, O.; Skancke, P. N. *Acta Chem. Scand.* **1961**, *15*, 711.

(39) Miller, F. A.; Capwell, R. J.; Lord, R. C.; Rea, D. G. *Spectrochim. Acta, Part A* **1972**, *28A*, 603. Rea, D. G. Ph.D. Thesis, Massachusetts Institute of Technology, Cambridge, 1954.

(40) Rathjens, G. W.; Freeman, N. K.; Gwinn, W. D.; Pitzer, K. S. *J. Am. Chem. Soc.* **1953**, *75*, 5634. Dows, D. A.; Rich, N. *J. Chem. Phys.* **1967**, *47*, 333. Aleksanyan, V. T.; Kuz'yants, G. M.; Lukina, M. Yu.; Zotova, S. V.; Vostokova, E. I. *J. Struct. Chem.* (*Engl. Transl.*) **1968**, *9*, 123. Aleksanyan, V. T. *Opt. Spectrosc.* (*Engl. Transl.*) **1970**, *29*, 574.

(41) Aleksanyan, V. T.; Antipov, B. O. *J. Mol. Struct.* **1982**, *89*, 15.

(42) Castelucci, e.; Miglionini, M. G.; Manzelli, P. *Acta. Crystallogr., Sect. A* **1972**, *A28*, 432.

(43) Lord, R. C.; Stoicheff, B. P. *Can. J. Phys.* **1962**, *40*, 725. Ueda, T.; Shimanouchi, T. *J. Chem. Phys.* **1968**, *49*, 470. Stone, J. M. R.; Mills, I. M. *Mol. Phys.* **1970**, *18*, 631. Miller, F. A.; Capwell, R. J. *Spectrochim. Acta, Part A* **1971**, *27A*, 947.

(44) Lord, R. C.; Nakagawa, I. *J. Chem. Phys.* **1963**, *39*, 2951.

(45) Banhegyi, G.; Fogarasi, G.; Pulay, P. *J. Mol. Struct.* **1982**, *89*, 1.

(46) Aleksanyan, V. T.; Antipov, B. G.; Ezernitzkaya, M. G. *Opt. Spectrosc.* (*Engl. Transl.*) **1981**, *50*, 1113.

(47) Annamalai, A.; Keiderling, T. A. *J. Mol. Spectrosc.*, in press.

(48) Polavarapu, P. L.; Nafie, L. A.; Benner, S. A.; Morton, T. H. *J. Am. Chem. Soc.* **1981**, *103*, 5349.

(49) Holzwarth, G.; Hsu, E. C.; Faulkner, T. R.; Moscowitz, A.; Mosher, H. S. *J. Am. Chem. Soc.* **1974**, *96*, 251.

Theory

In the FPC model,[6,7] partial charges are assigned to each atom, fixed at the nuclear positions and allowed to move along a normal coordinate. The underlying concept of this model is that the contribution of each atom to the dipole moment derivative is, in part, represented by the motion of a single effective charge which accounts for the nuclear charge and the average electron density around it. The major approximations are thought to be the constant magnitude of the charges, i.e., neglect of currents in the bonds, and the restriction to perfect correlation of the electron and nuclear motion. Schellman[6] has shown that, in first order, such a model generates dipolar (D^k) and rotational (R^k) strengths of the form

$$D^k = (\hbar/2\omega_k)|\sum_i q_i \mathbf{s}_i{}^k|^2 \tag{1}$$

$$R^k = (\hbar/4c)\sum_{i<j} q_i q_j(\mathbf{R}_{ij}\cdot\mathbf{s}_i{}^k \times \mathbf{s}_j{}^k) \tag{2}$$

where the q_i represents the effective charges, $\mathbf{R}_{ij}$ is the vector from atom i to j, and $\mathbf{s}_i{}^k$ is the Cartesian displacement vector for the normal mode of frequency ω_k. These formulas are quite simple to couple to normal coordinate calculations in a Cartesian basis and can be implemented in an internal coordinate-based calculation by use of the appropriate **B** matrix.[51] In these calculations, the GMAT and FPERT programs of Schachtschneider[52] have been modified to perform FPC calculations as well as the conventional normal coordinate calculations. The programs were checked against our previously developed Cartesian-based FPC routines.[13] Cartesian forms of the normal modes in the internal basis were calculated by using a procedure discussed by Levin and Pearce which, additionally, automatically treats redundant coordinates.[53]

Nafie and Walnut,[9] in the LMO model, have attempted to explicitly account for the contribution of the electrons in a manner such that their motion is not rigidly correlated to that of the nuclei. In their approach, molecular orbitals are calculated for molecular geometries in which all the nuclei are displaced along each normal coordinate of interest. Calculations are usually done for both positive and negative displacements. This has been referred to as the finite nuclear displacement (FND) method.[32] The molecular orbitals are then localized, and orbital centroids are obtained. The dipolar and rotational strengths are expressed in the LMO model with the following equations:[10]

$$D^k = \frac{\hbar e^2}{2\omega_k}\left|\sum_i Z_i \mathbf{s}_i{}^k - \sum_m \boldsymbol{\sigma}_m{}^k\right|^2 \tag{3}$$

$$R^k = \frac{\hbar e^2}{4c}[\sum_{i<j} Z_i Z_j(\mathbf{R}_{ij}\cdot\mathbf{s}_i{}^k \times \mathbf{s}_j{}^k) + \sum_{m<n} \mathbf{r}_{mn}\cdot\boldsymbol{\sigma}_m{}^k \times \boldsymbol{\sigma}_n{}^k - \sum_{i,m} Z_i(\mathbf{d}_{im}\cdot\mathbf{s}_i{}^k \times \boldsymbol{\sigma}_m{}^k)] \tag{4}$$

where Z_i now represents the atomic numbers, $\mathbf{s}_i{}^k$ is again the Cartesian normal coordinate vector, and $\boldsymbol{\sigma}_m{}^k$ is the displacement vector for the centroids of the orbitals m for the normal modes k. The distance vectors $\mathbf{R}_{ij}$, $\mathbf{r}_{mn}$, and $\mathbf{d}_{im}$ refer to the equilibrium configuration in which i and j refer to nuclei while m and n designate orbital centroids.

The $\mathbf{s}$ vectors were obtained by using the Schachtschneider programs[52] as in the FPC method. The LMO calculations were then carried out with the FND method by using CNDO-based programs as kindly supplied to us by Polavarapu.[31] It might be noted that the localization scheme used[9] avoids the fundamental problems that arise for calculating infrared intensities in the Born–Oppenheimer approximation.[54] It does not, however, explicitly include the vibronic corrections shown to be important beyond this level of approximations.[55]

Experimental Section

All samples used were prepared and purified at the University of Missouri—St. Louis. The trans (*dl*) and cis isomers of dideuteriocyclobutane were prepared by reductive deuteration of diethyl fumarate and diethyl maleate as previously described.[56] The trans (1*R*,2*R*) and (1*S*,2*S*) isomers were prepared from chiral 2,3-dibromo-2,3-dideuteriobutane-1,4-diol as previously described.[57] The resulting cyclobutane samples had a 1% d_0 and 14% d_1 impurity, as determined mass spectrometrically. Additionally, the samples contained a trace of water. While these impurities may have a small effect on the quantitative $\Delta A/A$ values measured, they will not qualitatively affect the VCD spectrum. The (1*S*,2*S*) sample had an enantiomeric excess of about 70% as compared to (1*R*,2*R*), which was determined both by relative VCD's and the optical purity of the starting reagents. Thus, VCD spectra measured on the (1*S*,2*S*) isomer were correspondingly corrected. The (1*R*,2*R*) sample was taken to be optically pure; its rotation of $[\alpha]^{20}_{\mathrm{D}}$ −0.015° ± 0.011° (neat) was previously reported.[57] The assessment of optical purity of the (1*R*,2*R*) sample is based on the optical purity of the starting 2,3-dibromo-2,3-dideuteriobutane-1,4-diol, the absence of any *cis*-1,2-dideuteriocyclobutane in the LAH reduction of the starting dibromide, and conversion of the acyclic precursor of the chiral dideuteriocyclobutane to 2,3-dideuteriosuccinic acid of known absolute configuration and rotation.[57] (Comparison of this small rotation with the large VCD reported in the next section further strengthens our suggestion that VCD monitoring of stereochemical change will be useful in such compounds.)

VCD and low-resolution (~12 cm^{-1}) absorption spectra of both gas and solution samples of the trans isomer in the C–H and C–D stretching regions were obtained on the UIC instrument described previously.[1] Fourier transform infrared spectra were obtained in the 4000–500-cm^{-1} range on gas-phase samples of both the trans and cis isomers at 4-cm^{-1} resolution with a Nicolet MX-5 instrument. Raman spectra were obtained on liquid samples of both isomers held in sealed ampols by using an instrument constructed in the UIC Physics Department. Excitation of 5145-A and resolution of 1 cm^{-1} were used.

For the absorption and VCD experiments, special cells for both gas- and solution-phase experiments were constructed to handle the high-vapor-pressure samples. To a 30-mm diameter by 70-mm path length Pyrex cell was added a Teflon stopcock inlet and a small side tube for condensing the cyclobutane. CaF$_2$ windows, sealed to the cell with Torr Seal (Varian), were used for the VCD experiments, and NaCl was used for the FT-IR measurements. A prime design constraint was the necessity of minimizing sample volume while maintaining a substantial path and avoiding artifact-generating reflections of the beam on the cell walls. The cell was filled by using a small vacuum line which was, for some experiments, coupled to a capacitance manometer. The line was filled with the cyclobutane vapor which, in turn, was condensed in the side tube of the cell, and the cell was then sealed. Pressure in the cell was estimated from the pressure in the line and the relative volumes of the cell and line. (Adequate VCD in the C–H stretching region could be obtained with pressures of ~12 torr. This corresponds to only ~2 mg of cyclobutane.) The ϵ and $\Delta\epsilon$ values reported here are only approximate but were also checked by weighing the condensed cyclobutane. The two methods agreed within 10–20%. Gas-phase VCD base lines were determined with the racemic sample and were found to closely approximate base lines measured with an empty cell.

To measure the solution-phase spectra a cylindrical brass cell with a path length of ~8 mm and a diameter of 25 mm was constructed. CaF$_2$ windows fixed onto the cell with Viton A o rings formed a vacuum-tight seal. A teflon stopcock and a glass stem were attached to the brass body via Kovar seals. After an appropriate amount of the sample was condensed into the glass stem, solvent was condensed from the vacuum line to fill the cell and the stopcock was closed. Within the period of measurement, the o rings were not found to be noticeably affected by either solvent or sample. Repeated spectra were found to be identical within the signal-to-noise limits of our experiment. The actual solution VCD were measured for the (1*S*,2*S*) isomer while that of the gas was run for both. For ease of comparison, the solution data presented here have been corrected to be appropriate for that of optically pure (1*R*,2*R*) isomers.

---

(50) Annamalai, A.; Keiderling, T. A. 37th Symposium on Molecular Spectroscopy, Columbus, OH, June 1982. Polavarapu, P. L. 38th Symposium on Molecular Spectroscopy, Columbus, OH, June 1983. Polavarapu, P. L.; Michalska, D. F. *J. Am. Chem. Soc.* **1983**, *105*, 6190.

(51) Wilson, E. B.; Decius, J. C.; Cross, P. C. "Molecular Vibrations"; McGraw-Hill: New York, 1955. Califano, S. "Vibrational States"; Wiley: New York, 1976.

(52) Schachtschneider, J. H. Technical Report No. 231–64; Shell Development Company: CA, 1964. Schachtschneider, J. H. Technical Report No. 57–65; Shell Development Company: Emeryville, CA, 1965.

(53) Levin, I. W.; Pearce, R. A. R. *Vib. Spectra Struct.* **1975**, *4*, 101.

(54) Mead, C. A.; Moscowitz, A. *Int. J. Quantum Chem.* **1967**, *1*, 243.

(55) Nafie, L. A.; Freedman, T. B. *J. Chem. Phys.* **1983**, *78*, 7108. Nafie, L. A. *J. Chem. Phys.*, in press.

(56) Chickos, J. S. *J. Org. Chem.* **1979**, *44*, 780.

(57) Chickos, J. S.; Bausch, M.; Alul, R. *Ibid.* **1981**, *46*, 3559.

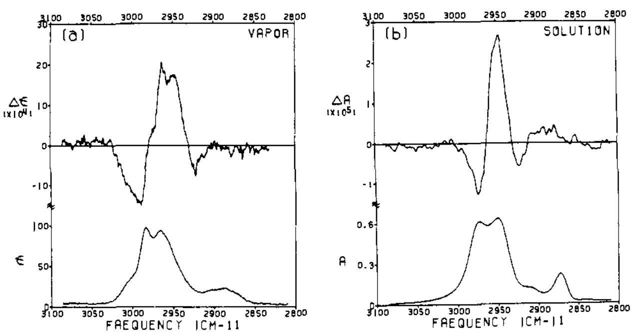

Figure 2. Absorption and VCD spectra of *trans*-1(*R*),2(*R*)-dideuteriocyclobutane in the C–H stretching region for vapor phase (a) and CCl$_4$ solution (b). Resolution, 11 cm^{-1}; (a) four scans at 10-s time constant; (b) six scans at 3-s time constant.

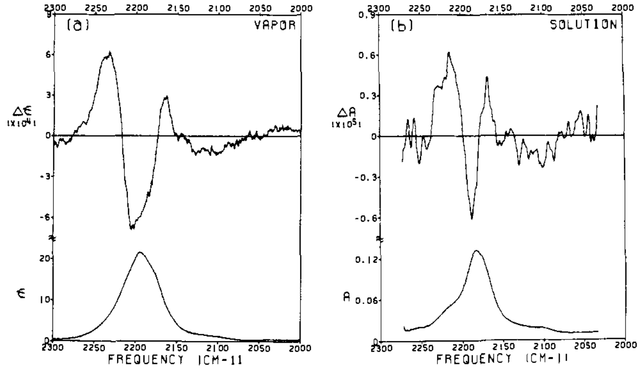

Figure 3. Absorption and VCD spectra of *trans*-1(*R*),2(*R*)-dideuteriocyclobutane in the C–D stretching region for vapor phase (a) and CCl$_4$ solution (b). Resolution, 12 cm^{-1}; (a) two scans and (b) six scans at 3-s time constant.

These spectra are reported as ΔA and A due to the difficulty in quantitatively determining and controlling concentration. Solution VCD base lines were obtained for just a CCl$_4$ solvent-filled cell. This can result in a shift of the VCD from the expected base line. The solution C–D stretching VCD data presented here have been appropriately corrected.

Results

The observed VCD and absorption spectra of *trans*-1(*R*),2-(*R*)-dideuteriocyclobutane in the gas phase and in CCl$_4$ solution are given in Figures 2 and 3 for the C–H and C–D stretching regions, respectively. Overall, the solution- and gas-phase VCD patterns are comparable. In the C–H VCD, a dominant sign pattern (−+−) is found in going from high to low frequency. However, the weak, broad positive signal in the solution spectrum centered at 2890 cm^{-1} is not observable in the gas-phase VCD. Near the single C–D stretching absorption maximum, a different VCD pattern (+−+) is observed with an additional broad negative band to low energy. The latter is probably due to combination bands.[3] The solution C–D stretching VCD is quite noisy because only a small quantity of the sample was available for measurement of this spectrum (note that the peak absorbance in Figure 3b is only ~0.15).

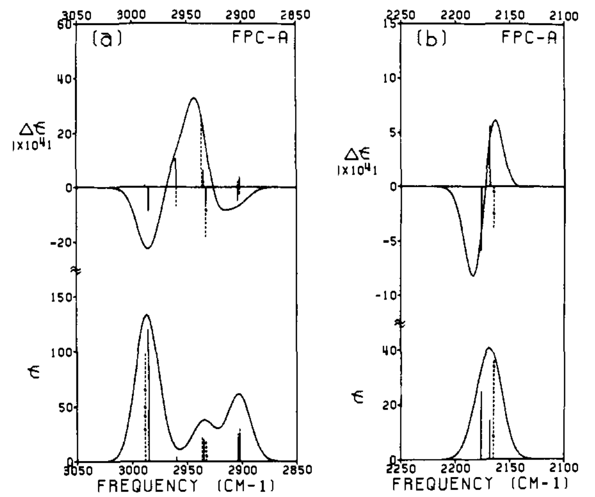

Figure 4. FPC-calculated absorption and VCD spectra of *trans*-1-(*R*),2(*R*)-dideuteriocyclobutane for L&N force field (FPC-A in Table I) for the C–H (a) and C–D (b) stretching modes. The ϵ and $\Delta\epsilon$ values are 50% of the sum for the equatorial and axial conformers (see Figure 1). The relative dipolar and rotational strengths are represented by vertical lines (—) for equatorial and (---) for axial conformers.

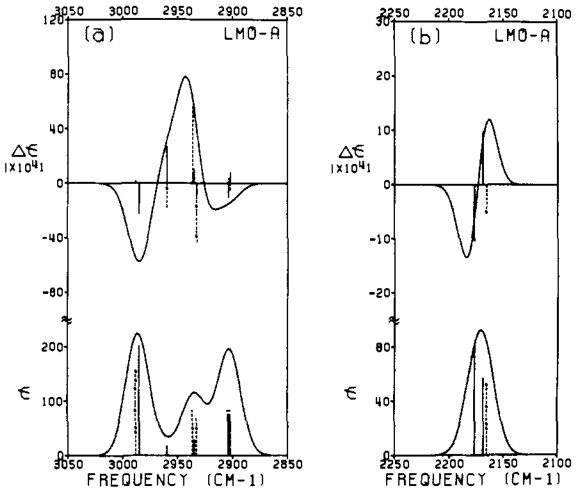

Figure 5. LMO-calculated absorption and VCD spectra for L&N force field (LMO-A in Table I), plotted as in Figure 4.

The $\Delta A/A$ values measured for the solution are higher than those found for the gas phase with this effect being slightly larger for the C–H stretches than for the C–D stretches. This magnitude change is consistent with the fact that considerable cancellation occurs in the C–H VCD due to overlap of many modes but that these bands are better resolved in solution. Additionally, the $\Delta\epsilon/\epsilon$ values for the C–D stretching region are somewhat larger than those for the C–H region. This is similar to the observation made by Polavarapu et al.,[48] though the $\Delta\epsilon/\epsilon$ value observed by these authors in the C–D stretching region is nearly 10^{-3} for *trans*-2,6-dideuteriocyclohexanone while the largest value we have measured here is only $\sim 10^{-4}$. Finally, we note that each spectral region evidences a gas-to-solution frequency shift of ~15 cm^{-1} to lower energy in the VCD for the first zero crossing. Not all bands are so shifted. In each case, the lower energy VCD feature ((−)-C–H, (+)-C–D) is at about the same frequency in each phase. This implies that the frequency separation of these modes is smaller in the solution phase. A shift to lower energy is normally expected upon solution.

In order to analyze these spectra we have carried out a number of FPC and CNDO-LMO VCD calculations using different force fields and, in the FPC case, different effective charges. Our initial force field choice was that of L&N[44] for which FPC and LMO results are presented in Figures 4 and 5, respectively. For Figure 4, the FPC charges were −0.278 |e| on C and +0.139 |e| on H(D). These gave an integrated C–H stretching absorption intensity approximately equal to the experimental value. In both cases the NMR-derived geometry of Meiboom and Snyder[37] was used. This is virtually equivalent to the best theoretical, equilibrium-corrected structure, aside from C–H bond length.[35] To carry out the FND for the LMO calculations, a distortion of ±0.02 A was used along each normal coordinate of interest.[11,12] In both figures, the calculated dipolar and rotational strengths of the equatorial conformer (Figure 1) are represented by solid vertical lines while those of the axial conformer are represented by dashed lines. The calculated $\Delta\epsilon$'s are represented by an envelope formed from the sum of corresponding Gaussian line shapes of 15-cm^{-1} half-width. For the sake of conservation of space, we have superimposed the contributions of the two conformers and only graphically represented the sum. The individual contributions are tabulated in Table I as FPC-A and LMO-A for the two separate calculations.

Table I. Calculated Fequencies and Dipolar and Rotational Strengths with Different Force Fields for the C–H and C–D Stretching Modes of the Two Conformers of *trans*-1(*R*),2(*R*)-Dideuteriocyclobutane[a]

FPC-A[b]			LMO-A[b]		FPC-B[c]			LMO-B[c]		FPC-C[d]			FPC-D[e]			LMO-D[e]		FPC-E[f]			approx. assign. and symmetry
ν	D	R	D	R	ν	D	R	D	R	ν	D	R	ν	D	R	D	R	ν	D	R	
Equatorial Conformer[g]																					
2169	1.84	12.08	6.49	18.77	2171	1.93	12.35	6.43	17.44	2178	1.60	10.14	2149	1.60	10.05	4.87	14.83	2159	1.66	10.23	sym C–D str A
2177	3.26	−12.44	9.47	−19.75	2188	3.53	−13.13	9.80	−19.04	2169	3.08	−10.05	2158	3.11	−10.72	7.54	−15.19	2151	3.17	−10.75	asym C–D str B
2904	2.20	−6.04	7.52	−12.68	2894	2.14	−3.80	7.22	−7.45	2937	2.05	−13.13	2900	2.14	−0.97	6.74	−4.42	2929	2.23	1.27	sym CH_2 str A
2902	2.60	4.53	7.56	9.50	2914	2.29	16.00	7.41	34.10	2928	2.20	3.26	2905	2.11	2.35	6.34	7.30	2922	2.14	−4.86	sym CH_2 str B
2933	0.15	−7.40	0.34	−13.44	2936	0.36	−9.78	0.98	−19.47	2947	0.09	−1.60	2945	0.23	−7.56	0.56	−14.18	2944	0.36	−4.83	sym C*–H str A
2935	2.05	7.18	2.91	11.93	2957	4.35	−2.57	6.14	−8.13	2955	1.96	6.37	2944	6.76	8.09	9.68	15.69	2949	2.66	11.99	asym C*–H str B
2960	0.42	12.11	1.83	31.65	2973	0.33	12.41	1.54	32.96	2969	0.33	13.59	2968	0.15	7.37	0.56	19.16	2954	0.00	1.93	asym CH_2 str A
2985	12.08	−10.11	20.60	−26.19	2986	10.05	−11.56	17.14	−30.51	2986	11.74	−8.78	2972	7.09	−8.88	10.67	−23.10	2961	11.17	−5.68	asym CH_2 str B
Axial Conformer[g]																					
2169	0.42	7.70	1.07	10.09	2171	0.51	8.45	1.17	10.02	2173	0.33	6.13	2173	0.42	6.91	0.96	9.67	2163	0.36	6.31	sym C–D str A
2165	1.69	−8.42	6.15	−9.94	2176	5.04	−9.51	6.45	−10.35	2171	4.26	−6.49	2162	4.38	−7.31	5.77	−9.12	2164	4.47	−6.64	asym C–D str B
2904	2.51	2.29	8.76	4.24	2894	2.14	4.26	7.35	8.69	2936	2.69	1.84	2900	1.75	1.15	5.38	4.40	2928	2.75	−4.53	sym CH_2 str A
2902	3.02	−3.44	8.99	−6.67	2912	5.13	6.31	15.00	16.00	2927	1.36	−4.77	2904	2.84	0.88	8.18	−1.39	2920	1.15	−2.66	sym CH_2 str B
2933	1.84	−21.25	7.08	−52.47	2936	1.96	−17.78	7.48	−43.22	2967	1.09	−24.18	2927	2.05	−15.88	6.54	−30.64	2936	1.27	−11.02	sym C*–H str A
2936	2.20	30.22	8.58	74.77	2961	0.78	17.57	3.33	44.58	2955	4.17	25.21	2936	3.65	16.60	7.89	33.71	2935	5.22	24.36	asym C*–H str B
2960	0.18	−8.24	0.89	−22.05	2973	0.42	−13.83	1.86	−35.60	2959	0.24	−3.26	2969	0.27	−11.74	1.11	−27.41	2953	0.18	−9.51	asym CH_2 str A
2988	9.93	0.69	16.30	2.27	2988	9.21	4.08	15.34	9.98	2983	8.82	5.40	2972	7.97	9.09	11.87	21.12	2960	8.06	3.44	asym CH_2 str B

[a] Empirical charges were used in FPC calculations with −0.278 |e| on C and +0.139 |e| on H(D) atoms; frequencies in cm^{-1}, dipolar strengths in 10^{-39} (esu·cm)^2, and rotational strengths in 10^{-44} (esu·cm)^2. [b] L&N force field, L&N symmetry coordinates for D_{2d} symmetry of C_4H_8 and experimental NMR geometry (ref 37). [c] L&N force field further refined by using a different assignment. [d] BFP ab initio scaled force field, BFP coordinates, and Cremer's ab initio geometry. [e] Ab initio based refined force field. [f] CNDO-scaled force field, L&N coordinates, and NMR geometry. [g] See Figure 1.

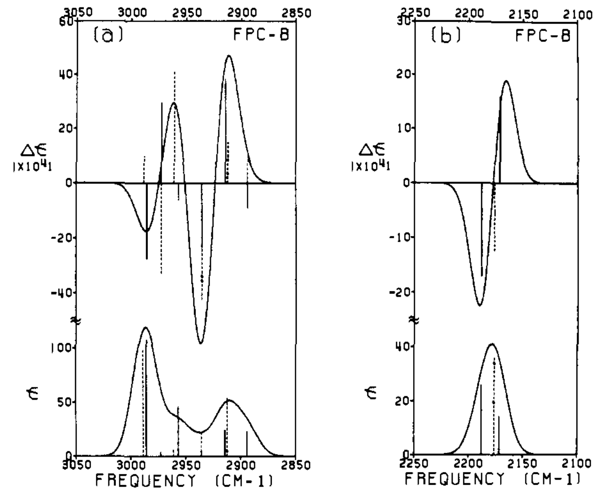

Figure 6. FPC-calculated absorption and VCD spectra for L&N-based refined force field (FPC-B in Table I), plotted as in Figure 4.

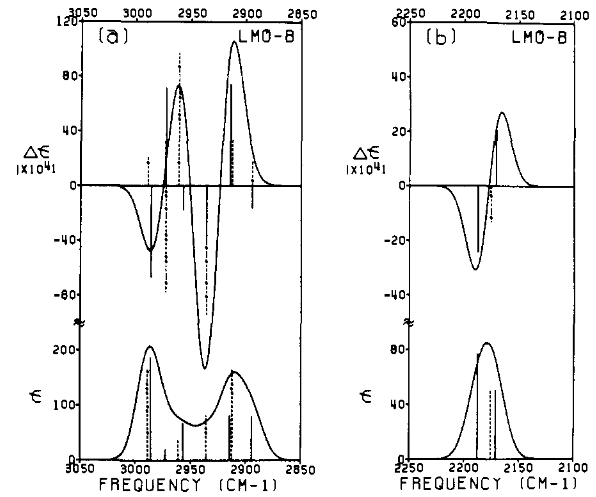

Figure 7. LMO-calculated absorption and VCD spectra for L&N-based refined force field (LMO-B in Table I), plotted as in Figure 4.

Both the LMO- and FPC-calculated VCD patterns (−+−) for the C–H region are in good qualitative agreement with the major features of the experimental spectrum. But in the C–D stretching region, the calculated patterns are significantly different from experiment. In both cases, the calculated VCD has a bisignate (−+) pattern whereas the experimental has a (+−+) pattern. Furthermore, the FPC- and LMO-calculated VCD and absorption curves are similar to each other. In the C–H region, the FPC-calculated $\Delta\epsilon$ values are ~1.5 times greater than found for the vapor experiment. This may be due to the line width used. $\Delta\epsilon/\epsilon$ for this FPC calculation lies above but close to the vapor values. The LMO values are about 2 times too large for ϵ and 4 times for $\Delta\epsilon$. $\Delta\epsilon/\epsilon$ for LMO-A is close to the solution values. In both calculations the proper frequency relationship between VCD and absorption features is seen.

In the second set of calculations, labeled FPC-B and LMO-B in Table I, we have used a force field derived by optimizing the fit to the revised C_4H_8 and C_4D_8 assignments.[39] The starting point for this optimization was the L&N force constants, but, for this calculation, the symmetry coordinates were reexpressed for the experimental, D_{2d}, puckered geometry. (The original L&N force field was determined by using a planar cyclobutane geometry.[44]) No additional force constants were considered.

The FPC-B and LMO-B results are graphically presented in Figures 6 and 7, respectively. The C–H stretching region VCD is less well fit than with the L&N force field. Although the calculated sign pattern, (−+−+) from high to low frequency, follows that seen in solution, the relative magnitudes are severely altered from Figures 4 and 5 and the experiment. The major

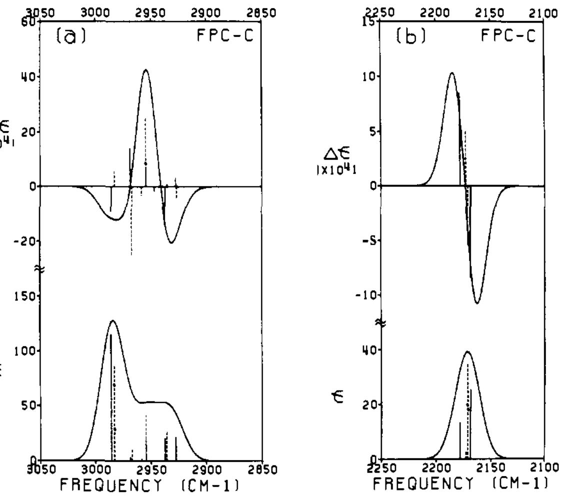

Figure 8. FPC-calculated absorption and VCD spectra for BPF ab initio scaled force field (FPC-C in Table I), plotted as in Figure 4.

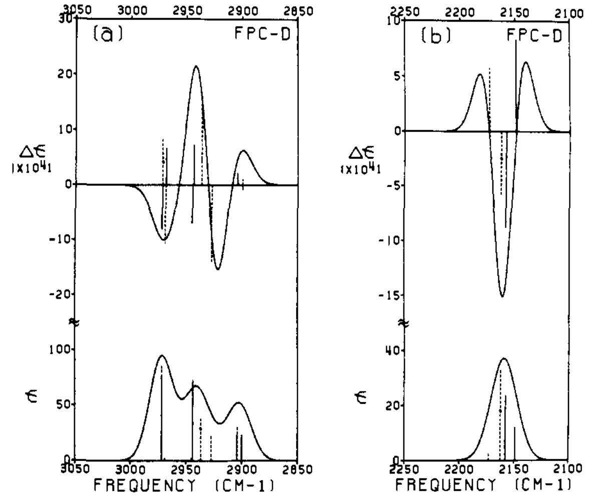

Figure 9. FPC-calculated absorption and VCD spectra for ab initio based refined force field (FPC-D in Table I), plotted as in Figure 4.

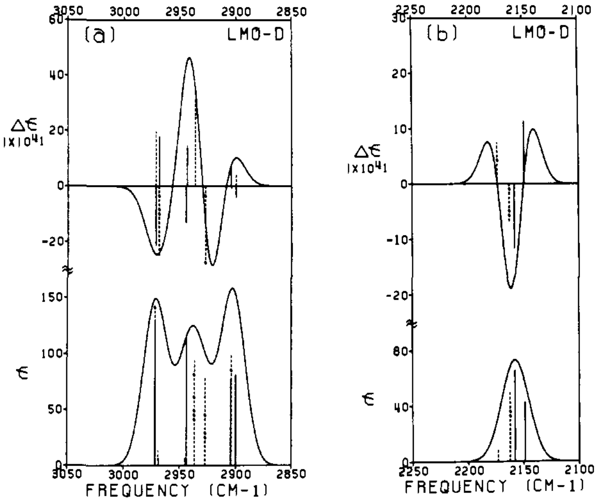

Figure 10. LMO-calculated absorption and VCD spectra for ab initio based refined force field (LMO-D in Table I), plotted as in Figure 4.

change is a dramatic increase in the VCD magnitude at lower frequencies which is correlated with an increase in the splitting of the modes in this region. As in A, the C–D stretching region yields a (−+) pattern and, aside from magnitudes, the LMO and FPC results are again qualitatively the same.

Our third set of calculations used the BFP ab initio force field[45] and is labeled C in Table I. We used a set of redundancy free internal coordinates instead of the symmetry coordinates of L&N. Since ab initio calculations tend to overestimate the diagonal force constants, a method of scaling and a set of optimized scale factors were developed by BFP. The diagonal and off-diagonal force constants were then obtained by using the following equations:[45,58]

$$F_{ii}^{sc} = C_i F_{ii} \qquad F_{ij}^{sc} = (C_i C_j)^{1/2} F_{ij} \qquad (5)$$

where the C_i's are scale factors.

On the basis of their force field, BFP have suggested some new assignments beyond those of Miller et al.[39] However, the BFP refinement of the scaling factors was quite limited in that the C–H stretching and ring puckering values were fixed, and no attempt was made to assign the C–H and C–D stretching modes. This was due to the complexity of the spectrum in this region which arises both from overlap of fundamentals and from interaction with overtone and combination bands.

We have refined all the scale factors further, particularly by considering different scale factors for CH_2 scissoring, rocking, and twisting modes, by including the C–H stretching frequencies as assigned by Miller et al.,[39] and by using Cremer's ab initio geometry.[36] This latter geometry was selected over that of BFP,[45] since it results from a larger basis set calculation. Such refinements did not improve the frequency fit to any considerable extent. This is mainly due to the constraint imposed on the force field because of the nature of scaling involved; i.e., the off-diagonal and diagonal scale factors are not independent. Both the BFP and our scale factors lead to similar FPC-calculated VCD and absorption spectra. Hence, only the plots corresponding to the original BFP scale factors are given in Figure 8 for data set FPC-C of Table I.

The calculated VCD in the C–H stretching region again has the (−+−) sign pattern as seen in set A and for the experimental spectrum. The resultant magnitudes of $\Delta\epsilon$ and ϵ are also very similar to those in Figure 4 (FPC-A). For the C–D stretching region VCD we now calculate a (+−) pattern which is just the reverse of that obtained for the calculations A and B above. While only two VCD features are obtained in the C–D stretching region, these, for the first time, reflect the sign pattern of the most intense experimental features.

In order to improve the ab initio force field, we next carried out another conventional force field refinement calculation considering the diagonal and off-diagonal constants independently. The vibrational frequencies of *cis*- and *trans*-1,2-dideuteriocyclobutanes measured in our laboratory[47] as well as those previously published for C_4H_8 and C_4D_8[39] were included in the refinement. The starting force field included the most significant ab initio force constants. The initial force field gave absorption and VCD plots similar to those in Figure 8 for FPC-C. Details of this normal coordinate analysis will be published separately.[47] The FPC-D and LMO-D results obtained with our final optimized force field[47] are graphically represented in Figures 9 and 10, respectively, and are detailed in Table I as set D. In the C–H region the calculated VCD with both theories has a (−+−+) pattern that quite satisfactorily resembles the experimental result. The FPC-calculated magnitudes also show improved agreement with experiment except for the lower frequencies. For the C–D region a (+−+) pattern is now seen which fits the experimental C–D VCD better than any of the previous sets of calculations, A–C. After optimization, the relative intensities in the C–H region have lost some of their agreement with experiment. This comparison of C–H patterns for D vs. C in a way parallels that for B vs. A. Optimization tends to spread the fundamentals, leading to consequent changes in their overlaps.

For the sake of comparison, we also used a CNDO-based force field[59] to perform FPC calculations. The program used is that from IIT, MADRAS,[60] which we have modified by including routines

---

(58) Blom, C. E.; Altona, C. *Mol. Phys.* **1976**, *31*, 1377; **1977**, *34*, 177.

(59) Pulay, P.; Torok, F. *Mol. Phys.* **1973**, *25*, 1153.

(60) Kanakavel, M.; Chandrasekhar, J.; Subramanian, S.; Singh, S. *Theor. Chim. Acta* **1976**, *43*, 185.

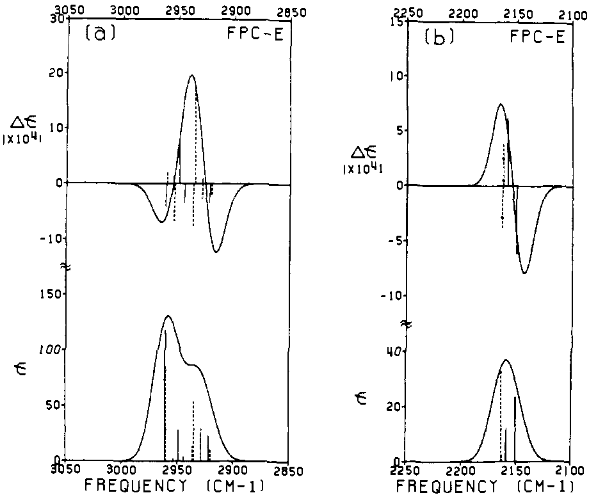

Figure 11. FPC-calculated absorption and VCD spectra for CNDO-scaled force field (FPC-E in Table I), plotted as in Figure 4.

to distort the molecule automatically and then to calculate the forces and force constants, all in a single run. To distort the molecule, the procedure suggested by Pulay et al.[61] was used. The diagonal and off-diagonal force constants were then scaled as given in eq 5. The stretching diagonal force constants are overestimated by a factor of 2–3 in the CNDO method, but the bending force constants are generally close to the experimental values. The scale factors were then refined by using the experimental frequencies and the L&N symmetry coordinates. Thus, the level of refinement is equivalent to that used for FPC-C. The FPC-E results (Table I) corresponding to this CNDO-based force field are represented in Figure 11. As we had hoped, the VCD and absorption patterns of FPC-E are similar to those obtained in calculation C where we used a scaled ab initio force field. However, the detailed rotational strengths in Table I for FPC-E show more variations from the pattern seen above than do any of the other calculations (see next section).

Discussion

The initial purpose of this work was to obtain an analysis of the relative effectiveness of the FPC and LMO models in fitting the VCD in C–H and C–D stretching regions for a simple saturated hydrocarbon. Additionally, we wished to examine the influence of force field and, in the case of FPC, effective charge selection. The strength of this work, as compared to previous FPC and LMO studies, is the near ideal nature of the molecule used. As such, we will first make some general comments regarding these two theoretical models and then discuss specific analyses of our data and calculations.

As is clear from the data in Figures 4–10 and Table I, there is no advantage in using the LMO model for cyclobutane over the FPC. This, in retrospect, is consistent with the previously published hydrocarbon VCD calculations where either the LMO and FPC results agree[11] or, in cases for which only FPC results are available, the FPC–VCD qualitatively resembles the experimental spectrum.[12,13] At this point, we would contend that the computationally simpler FPC model is satisfactory for such C–H stretching VCD. On the other hand, this assertion does not apply to molecules and, in particular, to normal modes which involve π electrons and lone-pair atoms. From the work of Freedman et al.,[29] it appears that in these latter cases, the LMO model is indeed superior to the FPC model.

However, our previous observations[13] that those molecules yielding conservative VCD in the C–H stretching region will be best fit by the FPC model remain valid. This is because conservative VCD results from dipolar coupling within the set of C–H stretches, and such coupling is well represented in the FPC. Nonconservative VCD indicates that other interactions may be important which may not be encompassed by the FPC. Clearly then molecules with a single C–H or C–D stretch would be poor candidates for FPC studies.

It is relevant to ask why these two, the FPC and LMO models, are so similar. Conceptually, the FPC appears to be a reasonable approximation for electron motion in saturated hydrocarbons. In other systems, particularly those with polarizable functional groups, the FPC will clearly be a poorer model since it cannot represent charge displacement on one atomic site induced by a nuclear displacement at another site. The LMO should, at some level, contain this effect.

Our results imply that the prime consideration for adequate representation of the VCD is a highly developed force field. However, it is possible that this implication is overstressed here. The opposite conclusion followed from our previous work by using crude force fields for six-member rings.[12,13] In fact, all the force fields we tested here gave a qualitative fit to the C–H stretching VCD, but only the quantum mechanical force fields (C–E) could be said to satisfactorily fit the C–D stretches. This improved fit to C–D stretches results solely due to a change in frequency of the normal modes for the two conformers which, in turn, results from off-diagonal force constants. As noted above, difficulty in interpreting C–D VCD is not uncommon due to overlapping combination bands.[3,48]

This brings us to an important general point. While our optimized force field yields LMO and FPC calculations that fit the C–D stretching region better, they fit the C–H regions worse. This seeming paradox may be due to the fact that all of our force fields are harmonic. As such, optimization of the force constants tends to compensate for anharmonic effects upon the observed frequencies. This, in turn, may lead to calculated normal modes which evidence more interaction than is warranted. In crowded spectral regions, overlap of the VCD features determines the overall line shape and is highly dependent on proper frequency determination. Rather than a change in the actual motion of the normal mode which leads to a change in R^k, this frequency overlap is the source of the main differences of the $\Delta\epsilon$ envelopes in our calculated spectra. That is why the force field became important where the two conformers must have slightly different frequencies to yield the observed C–D stretching VCD (see below).

Our previous studies have successfully used quite crude force fields for the study of C–H stretching VCD. In a sense, calculation A is of this nature. The qualitative line shape is preserved since the force fields are representing the motion of interest in a simple, yet apparently accurate, fashion. Our expectation is that simple force fields will be less useful for lower energy modes where more complex mixing is expected. If anharmonic effects are not dominant, the C–D stretching results presented above may be seen as evidence in favor of this assertion.

Another point might be made regarding this LMO and FPC comparison. Both the ϵ and $\Delta\epsilon$ values in the LMO model are 2–4 times higher than that found for the vapor, depending on the force field used. The $\Delta\epsilon/\epsilon$ values remain satisfactory, especially considering the variation between vapor and solution results. In general, previous LMO calculations[10,11,29] did show the LMO values to be higher than corresponding FPC values, with those of alanine[29] showing the same magnitude discrepancy from experiment as seen here. In that work, the difference of theory and experiment was attributed to solvent–solute interaction with alanine in D_2O giving much lower absorbances than in CCl_4. While we have seen similar solvent effects between CS_2 and CCl_4 for VCD of a borate complex,[62] the cyclobutane spectra here are measured in the gas phase, for which the LMO method should be appropriate. Thus, it would seem that the LMO, in some minor way, overcompensates for charge redistribution effects.

Beyond these general points, it is useful to scrutinize the data in Table I in some detail to evaluate the source of the large components observed in the VCD. We have attempted to order the normal modes in a consistent manner such that modes of

---

(61) Pulay, P.; Fogarasi, G.; Pang, F.; Boggs, J. E. *J. Am. Chem. Soc.* **1979**, *101*, 2550.

(62) Heintz, V. J.; Freeman, W. A.; Keiderling, T. A. *Inorg. Chem.* **1983**, *22*, 2319.

Table II. Frequencies and Dipolar and Rotational Strengths Obtained from FPC Calculations by Using CNDO-Scaled Charges[a]

FPC-A[b]			FPC-B[c]			FPC-D[d]		
ν	D	R	ν	D	R	ν	D	R
				Equatorial Conformer[e]				
2169	4.53	29.01	2171	4.47	28.62	2149	4.20	28.50
2177	9.09	−29.74	2188	8.97	−30.70	2158	9.15	−30.61
2904	3.47	18.99	2894	3.56	20.08	2900	4.02	29.16
2902	4.77	−18.93	2914	4.56	−10.02	2905	6.07	−25.33
2933	0.06	1.42	2936	0.06	−1.15	2945	0.00	−0.27
2935	0.18	−4.95	2957	0.69	−10.05	2944	0.72	0.39
2960	2.48	28.32	2973	2.42	30.10	2968	1.69	23.00
2985	8.82	−24.00	2986	8.42	−27.08	2972	6.91	−25.51
				Axial Conformer[e]				
2169	0.06	1.84	2171	0.18	2.57	2173	0.03	1.15
2165	0.69	−1.87	2176	0.97	−2.67	2162	0.45	−1.12
2904	4.38	−26.90	2894	3.56	−19.89	2900	3.11	−22.85
2902	5.22	24.24	2912	7.49	51.26	2904	6.19	35.74
2933	5.89	−58.19	2936	5.68	−49.45	2927	5.58	−51.29
2936	9.75	73.09	2961	6.91	40.51	2936	12.50	45.10
2960	1.66	−20.71	2973	2.69	−32.51	2969	2.51	−31.03
2988	10.90	4.53	2988	11.20	10.14	2972	7.28	24.33

[a] Charges: −0.278 |e| on C, +0.252 |e| on equatorial H(D), and +0.026 |e| on axial H(D) atoms (scale factor used in 14.7); frequencies in cm^{-1}, dipolar strengths in 10^{-39} (esu·cm)^2, and rotational strengths in 10^{-44} (esu·cm)^2. [b] L&N force field. [c] L&N-based refined force field. [d] Ab initio based refined force field. [e] See Figure 1.

predominately the same type of motion (as determined from the potential energy distribution) and of the same symmetry would be in similar positions for each calculation in the table. The overall ordering is in terms of increase in frequency and alternating symmetry, A or B. Thus, for each calculation and each conformer the C–D stretches occur first in the table and the asymmetric CH_2 stretches occur last. When presented in this manner, a startling consistency in signs for a given mode becomes clear.

First, for each pair of LMO and FPC calculations, the rotational strengths of identical modes have the same sign except for one, and, in that case, the R^k values are very small. Such a comparison serves to further confirm our earlier qualitative comments about the similarities of the FPC and LMO models for cyclobutane. Furthermore, the sign pattern seen for the FPC-A calculation for both isomers is violated only eight times in all of the other calculations, and three of those occur in the FPC-E calculation based on the CNDO force field. This high correlation appears to result from the unusual purity of C–H and C–D stretching modes. The primary nature of the resulting normal modes is fixed by symmetry constraints; thus, the force field seems to cause only minor mixing and frequency shifts.

Other systematics are also evident in terms of sums of rotational strengths for modes of similar energy belonging to the same symmetry representation. For example, symmetric CH_2 and C*–H stretches of B symmetry are within 30–40 cm^{-1} of each other. For the FPC calculations (A–E) the R^k values of both of these modes are positive in sign with some exceptions for the two conformations. But more importantly, for each calculation, considering both conformers, the rotational strengths of the four possible modes sum to a positive value in the range of 28–38 × 10^{-44} (esu·cm)^2. Though modes of the same symmetry mix differently in each calculation, the mixing mainly occurs between near-degenerate modes. Such limited interaction tends to give a constant integrated VCD. This, in turn, is the source of the stability of line shape broadened VCD calculated for these transitions. Similar arguments can be applied to the analogous set of A symmetry modes, but the effect is smaller.

It is interesting to note that the C*–H modes mix more strongly with the symmetric rather than asymmetric CH_2 stretching modes. A similar result was found in our analysis of CH_3–C*–H containing molecules.[19,26] In those calculations, the symmetric CH_3 stretching mode strongly mixed with that of the C*–H, but the respective asymmetric CH_3 modes did not. This resulted in a large monosignate contribution to the VCD at lower energy than the bisignate VCD due to the asymmetric stretches. In a sense, similar results occur in the cyclobutane VCD. The asymmetric CH_2 stretches lie higher in energy than the other modes. To lower energy lie the composite C*–H and symmetric CH_2 modes, opposite in sign for the A and B symmetries. This alternation in sign provides much of the observed C–H VCD in the 2900–2970-cm^{-1} region.

On the other hand, the asymmetric CH_2 modes have the opposite sense for the two conformers. That is, for the equatorial conformer, the VCD of the A mode is always positive and B is always negative, while, for the axial, A is negative and B is positive. This sign flip is what we expect from the relative chiralities of the CH_2CH_2 groups in the two conformers. As discussed in the introduction, the bisignate VCD predicted for the individual conformers is the expected result of dipolar coupling.[10-18] However, the resultant VCD is not conservative and, thus, evidences mixing with C*–H modes. This is most evident in the scaled ab initio force field calculation, FPC-C. For these asymmetric CH_2 stretches, the B mode is higher in energy than the A, and the A and B modes, respectively, have nearly the same frequency in each conformer. These relationships lead to a cancellation of their dipolar coupling contributions and leave a net monosignate negative VCD due to coupling to the rest of the C–H stretches. This then is the source of the high-energy negative VCD seen in the C–H stretching region.

In the C–D stretching region, we again calculate VCD dominated by dipolar coupling. However, in this case, the C–D bonds in both conformers have the same chirality and give rise to R^k's of the same sign, A positive and B negative. This is the source of the simple bisignate shapes seen in Figures 4–8. The sign change seen in Figures 8 and 11 and the more complex spectra in Figures 9 and 10 are due to a change in the relative frequencies of the A and B modes, particularly for the equatorial conformer. In the case of the optimized ab initio force field (D), the triple-peak pattern, which is the best fit we have obtained to the experimental C–D VCD, results from a large frequency difference between the A modes in the equatorial and axial conformers. In other words, the triple-peak pattern calculated in Figures 9 and 10 for the C–D stretches is due to the offset overlap of a (+ −) pattern for one conformer with a (− +) for the other. In all cases the C–D VCD is nearly conservative, indicating a low level of mixing with other modes.

In addition, the C–D VCD can be compared to the C*–H VCD. Since these pairs of bonds have opposite chirality, we expect their coupled modes to have opposite VCD. This is borne out in our calculations where the C–D A mode is positive and the C*–H A mode is negative. As indicated above, the reverse signs hold for the respective B modes. This opposite handedness is in some part responsible for the opposite sign pattern of the C–H and C–D VCD. However, without detailed accounting for the frequencies of the individual modes, such a rationale is not useful. For example, in this case, the symmetric CH_2 modes in each conformer occur at nearly the same frequencies so that much of their contribution to the VCD cancels, but the C*–H labeled modes are more shifted in frequency between conformers which leads to their dominating the lower frequency part of the C–H stretching region. This, again, is the nature of the force field dependence we are observing. When this fundamental limitation is kept in mind, it seems that the calculations can be viewed as being in very good agreement with the experiment subject to minor shifts in frequency. At this level, VCD could be seen as a major additional constraint in conventional force field development since the patterns observed are much more sensitive to normal mode frequencies and symmetries than is the absorption spectrum in such spectrally crowded regions.

As well as an analysis of the applicability of the LMO and FPC models and a study of their force field dependencies, we have also attempted to study the effect of charge choice on the FPC results. The results in Table I for FPC calculations all used a charge distribution that treats the axial and equatorial hydrogens and deuteriums equivalently. In this model the charge magnitudes were scaled such that the sum of the calculated dipolar strengths matched the integrated experimental values. In this approach, the $\Delta\epsilon$ values also come out to be in satisfactory agreement with experiment. This equivalent charge distribution is not seen in the population analysis of a CNDO calculation. Such a method of determining charge would indicate that the axial values should be 0.026 $|e|$ and the equatorial values should be 0.252 $|e|$ to effect the same scaling. FPC calculations using this charge distribution show more detailed deviations from the systematics of Table I. However, the VCD envelope found for each region is qualitatively the same as that seen in Figures 4, 6, 8, and 9. This consistency again results from summed rotational strengths, being much more consistent than those of individual modes. This is particularly evident from summing A and B symmetry C*–H and symmetric CH_2 stretch R^k values (Table II). For this CNDO charge distribution, the two conformers tend to have large VCD's that cancel each other, while the equivalent charge distribution used in the calculations reported in Table I led to both conformers having smaller R^k's which, however, added constructively. Charge effects then could lead to changes in the high-resolution VCD but, for cyclobutane, do not seem to be important in our realistically broadened VCD plots.

Two other related points deserve comment. The equivalent charge distribution was chosen because it gave a significantly better representation of the absorption line shape in the C–H region. In most of our previous studies,[12,13] the FPC-calculated absorption did not adequately reflect the distribution of dipolar strength between asymmetric and symmetric CH_2 and CH_3 modes. This is also true for these calculations, but the situation is much worse when scaled CNDO charges are used. In this latter case, the symmetric CH_2 modes have too much intensity. We feel that the large difference in the magnitude of the charge between the axial and equatorial hydrogens must be an artifact of the CNDO method. It might be noted that the FPC results consistently calculate the ϵ and $\Delta\epsilon$ values for C–D stretching to be much higher than found experimentally. This appears to be due to a line-width difference in the C–H and C–D regions.

With the above in mind, it is very interesting to note how similar the FPC and LMO results are (aside from the overall magnitude). Since the LMO uses the same CNDO method that gives rise to the unusual charge distribution above, we might conclude that redistribution effects serve to counteract the static charge distribution.

Conclusion

In summary, we have shown that the LMO and FPC models give equivalent fits to the C–H and C–D stretching mode VCD of *trans*-1,2-dideuteriocyclobutane. Improved fit can be obtained by improving the force field, but this is primarily due to change in the frequencies of individual modes rather than in their fundamental nature. As such, it would seem that the basic sense of the calculated rotational strengths is not as strongly dependent upon force fields as are the frequencies. However, in crowded spectral regions, it is imperative that both effects be accounted for to fit VCD spectra accurately. Thus, it seems that the FPC will remain a useful qualitative theoretical model for C–H stretching VCD within the constraints of conservative spectra and moderate overlap of modes. Furthermore, we feel that this molecule, dideuteriocyclobutane, will provide a hydrocarbon standard for testing further theoretical models. Extension of these studies to the mid-infrared region should further test the applicability and force field dependence of the FPC model. Such studies are underway in our laboratory.

Acknowledgment. We gratefully acknowledge the National Science Foundation (CHE81-04997) and the National Institutes of Health (GM-30147) for support of this research. We thank Professor L. Abels for assistance in obtaining the Raman spectra and the Nicolet Corp. for loan of an FT-IR spectrometer. We especially thank Professor P. Polavarapu for allowing us to use his LMO program and instructing us in its use and Professors J. Overend and L. Nafie for helpful conversations.

Registry No. *trans*-1,2-Dideuteriocyclobutane, 75156-31-9.

Mechanism for Forming Hydrogen Chloride and Sodium Sulfate from Sulfur Trioxide, Water, and Sodium Chloride

Alfred B. Anderson

Contribution from the Chemistry Department, Case Western Reserve University, Cleveland, Ohio 44106. *Received February 21, 1984*

Abstract: A molecular orbital study of sodium sulfate and hydrogen chloride formation from sulfur trioxide, water, and sodium chloride shows no activation barrier, in agreement with recent experimental work of Kohl, Fielder, and Stearns. Two overall steps are found for the process. First, gas-phase water reacts with sulfur trioxide along a pathway involving a linear O···H···O transition state yielding closely associated hydroxyl and bisulfite which rearrange to become a hydrogen sulfate molecule. Then the hydrogen sulfate molecule transfers a hydrogen atom to a surface chloride in solid sodium chloride while an electron and a sodium cation simultaneously transfer to yield sodium bisulfate and gas-phase hydrogen chloride. This process repeats. Both of these steps represent well-known reactions for which mechanisms have not been previously determined.

Sodium sulfate is a product of the reaction of combustion gases with solid sodium chloride and is, in its molten state, a powerful corrosive agent against protective oxide films on turbine blades,[1] leading to failure by "hot corrosion".[2] Recently Anderson, Hung,

0002-7863/84/1506-6262$01.50/0